J. Fluid Mech. (1982), *vol.* 114, *pp.* 315–330
Printed in Great Britain

Instabilities of finite-amplitude water waves

By JOHN W. McLEAN

Fluid Mechanics Department, TRW Defense and Space Systems Group,
Redondo Beach, California, CA 90278

(Received 30 December 1980 and in revised form 13 May 1981)

A numerical investigation of normal-mode perturbations of a finite-amplitude Stokes wave has revealed regions of instability lying near resonance curves given by the linear-dispersion relation. It is found that, for small amplitude, the dominant instability is two-dimensional (of Benjamin–Feir type) but, for larger amplitudes, the dominant instability becomes a three-dimensional perturbation. Results are compared with recent experimental observations of steep wave trains.

1. Introduction

The stability of a uniform train of deep-water waves has been the subject of many investigations. For weakly nonlinear waves, perturbation methods have shown that the wave train is unstable to modulational (long-wavelength) perturbations (Lighthill 1965; Benjamin & Feir 1967). A numerical investigation (Longuet-Higgins 1978*a*) has extended these results to large-amplitude waves and finite-wavelength modulations, but the analysis was confined to perturbations having a wavelength that is a rational multiple of the unperturbed wave. All these studies dealt with two-dimensional perturbations. The effect of three-dimensional perturbations has been studied in two small-amplitude approximations, the nonlinear Schrödinger equation (Zakharov 1968), and the Zakharov equation (Crawford *et al.* 1981). The results based on the Zakharov equation indicate that, for small amplitude, bands of instability lie near resonance curves deduced from the linear-dispersion relation – Phillips' 'figure 8' (Phillips 1960).

In this paper, we give details of a numerical investigation of the stability of finite-amplitude deep-water waves to infinitesimal three-dimensional perturbations of arbitrary wavelength based on the inviscid water-wave equations, and extend the results described by McLean *et al.* (1981). The results of Benjamin & Feir (1967) and Crawford *et al.* (1981) are recovered when the unperturbed wave has small amplitude. For two-dimensional subharmonic perturbations of finite-amplitude waves, the results agree with those of Longuet-Higgins (1978*a*).

The present investigation shows that the resonance given by Phillips' 'figure 8' is only the first of a family of resonance conditions. The instability associated with the 'figure 8' is the dominant one for small waves, but for sufficiently steep waves the instability associated with the next-order resonance becomes dominant. For the latter instability, the largest growth rates always occur for with fully three-dimensional perturbations of the basic wave train. These instabilities give rise to three-dimensional wave patterns in agreement with recent experimental results (Su 1981).

2. The governing equations

We consider surface gravity waves on an inviscid, irrotational, incompressible fluid of great depth. In a frame of reference moving with constant speed C (which will be taken as the speed of the unperturbed wave), the basic equations are

$$\left.\begin{aligned} &\nabla^2\phi = 0, \quad -\infty < z < \eta, \\ &\phi \sim -Cx \quad \text{as} \quad z \to -\infty; \end{aligned}\right\} \tag{1}$$

$$\left.\begin{aligned} &\phi_t + \eta + \tfrac{1}{2}(\phi_x^2 + \phi_y^2 + \phi_z^2) = \tfrac{1}{2}C^2 \\ &\eta_t + \phi_x\eta_x + \phi_y\eta_y - \phi_z = 0 \end{aligned}\right\} \quad \text{on} \quad z = \eta; \tag{2}$$

in which $\phi(x, y, z, t)$ is the velocity potential, $z = \eta(x, y, t)$ is the free surface, and C is the phase speed of the unperturbed wave. Without loss of generality, the gravitational acceleration has been taken to be unity, and the unperturbed wave has wavelength $\lambda = 2\pi$. These equations admit steady solutions of the form

$$\left.\begin{aligned} \eta &= \bar{\eta}(x) = \sum_1^\infty A_n \cos nx, \\ \phi &= \bar{\phi}(x, z) = -Cx + \sum_1^\infty B_n \sin nx\, e^{nz}, \end{aligned}\right\} \tag{3}$$

where the Fourier coefficients A_n, B_n and the phase speed C are functions of the wave steepness h/λ, where h is the crest-to-trough height.

We consider the stability of these two-dimensional steady waves to an infinitesimal three-dimensional disturbance. Let

$$\eta = \bar{\eta} + \eta', \quad \phi = \bar{\phi} + \phi';$$

it is assumed that $\eta' \ll \bar{\eta}$ and $\phi' \ll \bar{\phi}$. To first order in the perturbations we obtain

$$\left.\begin{aligned} &\nabla^2\phi' = 0, \quad -\infty < z < \bar{\eta}; \\ &\left.\begin{aligned} &\phi_t' + \eta' + \bar{\phi}_x\phi_x' + \bar{\phi}_z\phi_z' + (\bar{\phi}_x\bar{\phi}_{xz} + \bar{\phi}_z\bar{\phi}_{zz})\,\eta' = 0 \\ &\eta_t' + \bar{\phi}_x\eta_x' + \bar{\eta}_x\phi_x' + (\bar{\phi}_{xz}\bar{\eta}_x - \bar{\phi}_{zz})\,\eta' - \phi_z' = 0 \end{aligned}\right\} \quad \text{on} \quad z = \bar{\eta}. \end{aligned}\right\} \tag{4}$$

We look for non-trivial solutions of (4) of the form

$$\left.\begin{aligned} \eta' &= e^{-i\sigma t}\, e^{i(px+qy)} \sum_{-\infty}^{\infty} a_j\, e^{ijx}, \\ \phi' &= e^{-i\sigma t}\, e^{i(px+qy)} \sum_{-\infty}^{\infty} b_j\, e^{ijx} \exp\{[(p+j)^2 + q^2]^{\frac{1}{2}} z\}, \end{aligned}\right\} \tag{5}$$

where p and q are arbitrary real numbers. The physical disturbance corresponds to the real part of (5). The perturbation has period $2\pi/q$ in the spanwise (y) direction, but is not strictly periodic in the propagation (x) direction unless p is rational.

Substitution of (5) into (4) gives

$$\left.\begin{aligned}(1+\overline{\phi}_x\overline{\phi}_{xz}+\overline{\phi}_z\overline{\phi}_{zz})\sum_{-\infty}^{\infty}a_j e^{ijx}+\sum_{-\infty}^{\infty}(i(p+j)\overline{\phi}_x+[(p+j)^2+q^2]^{\frac{1}{2}}\overline{\phi}_z)\\ \times b_j e^{ijx}e^{[\,]^{\frac{1}{2}}\eta}=i\sigma\sum_{-\infty}^{\infty}b_j e^{ijx}e^{[\,]^{\frac{1}{2}}\eta},\\ \sum_{-\infty}^{\infty}[\overline{\phi}_{xz}\overline{\eta}_x-\overline{\phi}_{zz}+i(p+j)\overline{\phi}_x]a_j e^{ijx}+\sum_{-\infty}^{\infty}(i(p+j)\overline{\eta}_x-[(p+j)^2+q^2]^{\frac{1}{2}})\\ \times b_j e^{ijx}e^{[\,]^{\frac{1}{2}}\eta}=i\sigma\sum_{-\infty}^{\infty}a_j e^{ijx}\end{aligned}\right\}\quad(6)$$

for $0\leqslant x\leqslant 2\pi$, where [ ] denotes $[(p+j)^2+q^2]$. Once the unperturbed wave $\overline{\eta},\overline{\phi}$ has been calculated, the coefficients in (6) may be evaluated, yielding an eigenvalue problem for σ with eigenvector $\{a_j,b_j\}$. Instability corresponds to $\mathscr{R}\sigma\neq 0$, since σ occurs in complex conjugate pairs, because the system described by (4) is real.

For $h/\lambda=0$, the unperturbed wave is $\overline{\eta}=0$, $\overline{\phi}=-x$, $C=1$. The eigenfunctions and eigenvalues are

$$\left.\begin{aligned}\eta_n' &= e^{-i\sigma_n t}e^{i[(p+n)x+qy]},\\ \sigma_n &= -(p+n)\pm[(p+n)^2+q^2]^{\frac{1}{2}}\end{aligned}\right\}\quad(7)$$

for each integer n. These eigenfunctions are merely infinitesimal waves with wavevector $\mathbf{k}=(k_x,k_y)=(p+n,q)$. The frequencies are $\sigma_n=-k_x\pm|\mathbf{k}|^{\frac{1}{2}}$ which corresponds to the linear dispersion relation in a frame of reference moving with speed 1. The choice of sign defines the propagation sense relative to the unperturbed wave. Note that there is a degeneracy in the choice of p since $\sigma_n(p,q)=\sigma_{n+1}(p-1,q)$. This degeneracy is artificial since the corresponding eigenfunctions are physically the same,† and is an artifact of the choice of the representation (5). We will label the eigenfunctions by (p,q) and specify the index of the dominant coefficient a_n. This will fix the dominant wavevector $\mathbf{k}=(p+n,q)$.

Nonlinear effects corresponding to $h/\lambda>0$ can lead to instability of these modes (i.e. complex eigenvalues) if the eigenvalues agree for different n and the same p and q in the linear approximation (7), i.e.

$$\sigma_{n_1}^{\pm}(p,q)=\sigma_{n_2}^{\pm}(p,q)\quad(8)$$

for some $[n_1,n_2]$ and choice of the propagation sense. The corresponding eigenvector will have dominant components with wavevectors $\mathbf{k}_1=(p+n_1,q)$ and $\mathbf{k}_2=(p+n_2,q)$. For gravity waves on deep water, the solution to (8) can be divided into two classes:

class I

$$\left.\begin{aligned}&\mathbf{k}_1=(p+m,q),\quad \mathbf{k}_2=(p-m,q),\quad \sigma_m^{+}(p,q)=\sigma_{-m}^{-}(p,q),\\ &[(p+m)^2+q^2]^{\frac{1}{2}}+[(p-m)^2+q^2]^{\frac{1}{2}}=2m;\end{aligned}\right\}\quad(9)$$

class II

$$\left.\begin{aligned}&\mathbf{k}_1=(p+m,q),\quad \mathbf{k}_2=(p-m-1,q),\quad \sigma_m^{+}(p,q)=\sigma_{-m-1}^{-}(p,q),\\ &[(p+m)^2+q^2]^{\frac{1}{2}}+[(p-m-1)^2+q^2]^{\frac{1}{2}}=2m+1.\end{aligned}\right\}\quad(10)$$

In the above, $m\geqslant 1$. These two classes account for all solutions to (8) apart from the degeneracy in the labelling as noted above. The curves described by (9) and (10) are

† The degeneracy can be removed by restricting p to the range $0\leqslant p<1$, but it turns out to be more convenient to allow for general p.

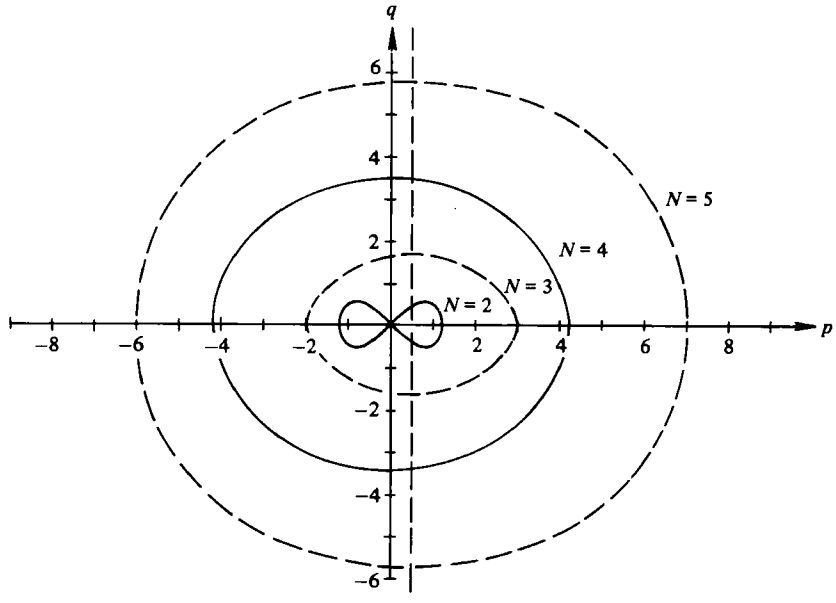

FIGURE 1. Resonance curves from the linear dispersion relation (equation 11). The index N labels the order of the interaction.

plotted in figure 1. Class I curves are symmetric about the origin, while class II curves are symmetric about $p = \frac{1}{2}$, $q = 0$.

The coincidence of the eigenvalues can alternatively be interpreted as resonance of two infinitesimal waves with a 'carrier' wave. Seen in a fixed frame of reference, the resonance condition is

$$\omega_1 = -\omega_2 + N\omega_0, \quad \mathbf{k}_1 = \mathbf{k}_2 + N\mathbf{k}_0, \tag{11}$$

where $\mathbf{k}_1 = (p' + N, q)$, $\mathbf{k}_2 = (p', q)$, $\mathbf{k}_0 = (1, 0)$, and $\omega_i = |\mathbf{k}_i|^{\frac{1}{2}}$, the linear-dispersion relation for gravity waves. Class I corresponds to N even, $m = \frac{1}{2}N$, $p' = p - m$; and class II corresponds to N odd, $m = \frac{1}{2}(N-1)$, $p' = p - m - 1$. The lowest-order resonance, $N = 2$, is Phillips' figure 8, and is expected to give rise to the dominant instability for small h/λ. Higher-order resonances are expected to give rise to additional instabilities.†

Previous analytical studies have been restricted to the lowest-order resonance ($N = 2$). The Benjamin–Feir analysis corresponds to $(h/\lambda) \ll 1$, $q = 0$, $p = O(h/\lambda)$. Stability analysis of the Schrödinger equation in three dimensions (Zakharov 1968) extends the result to $q \neq 0$. The Zakharov equation extends these results to larger values of h/λ (Crawford *et al.* 1981), but does not contain the higher-order resonances.

3. Numerical treatment

The computations consist of two parts, calculation of the unperturbed wave $\overline{\eta}, \overline{\phi}$ and solution of the eigenvalue problem. Accurate solutions for the two-dimensional Stokes wave have been obtained by Schwartz (1974), Cokelet (1977), Longuet-Higgins

† Zakharov (1968) suggests that these resonances lead to growth rates of order $(h/\lambda)^N$, but only shows this for $N = 2$.

(1978*b*), Chen & Saffman (1980), Saffman (1980), and others. For our purposes it proved convenient to recalculate the unperturbed wave by solving for x and z as functions of the velocity potential ϕ and the stream function ψ, as was done by Saffman (1980). In these variables, the unperturbed surface is a streamline ($\psi = 0$), and is given parametrically by

$$x = x(\phi) = \phi/C + \sum_1^\infty \frac{H_n}{n} \sin\frac{n\phi}{C}, \quad z = z(\phi) = \frac{H_0}{2} + \sum_1^\infty \frac{H_n}{n} \cos\frac{n\phi}{C}. \tag{12}$$

It has been shown (Longuet-Higgins 1978*b*) that the free-surface boundary condition (Bernoulli equation) can be written as a quadratic equation in the unknowns $\{H_n\}$:

$$\int_0^{2\pi C} e^{in\phi/C} z(x_\phi + iz_\phi)\, d\phi = -\pi C^2 \delta_{0n}. \tag{13}$$

Substitution of (12) into (13) yields the system

$$\left.\begin{aligned} H_0 + \sum_{n=1}^\infty \frac{H_n^2}{n} &= -C^2, \\ H_l\left(H_0 + \frac{1}{l}\right) + \sum_{n=1}^{l-1} \frac{H_n H_{l-n}}{n} + \sum_{n=1}^\infty \frac{H_n H_{l+n}}{n} &= 0, \quad 1 \leqslant l < \infty. \end{aligned}\right\} \tag{14}$$

This system is truncated at L Fourier modes and solved in double precision by Newton's method for each value of the wave steepness. For $h/\lambda \leqslant 0{\cdot}10$, $L = 100$ was used, with the last Fourier coefficient less than 10^{-13} in magnitude. As the steepness increases, it is necessary to use more modes to describe adequately the unperturbed wave. For the highest wave considered here $h/\lambda = 0{\cdot}1305$, $L = 300$ was used, with the last coefficient approximately 10^{-9} in magnitude. Wave properties such as the wave speed have been compared with previous calculations (Cokelet 1977), and the results agree to six significant figures.

Once the unperturbed wave is calculated, we return to Cartesian co-ordinates to compute the coefficients in (6). Using the fundamental relations

$$\left.\begin{aligned} \phi_x x_\phi + \phi_z z_\phi = 1, \quad \psi_x x_\phi + \psi_z z_\phi = 0, \\ \phi_x x_\psi + \phi_z z_\psi = 0, \quad \psi_x x_\psi + \psi_z z_\psi = 1, \end{aligned}\right\} \tag{15}$$

and the Cauchy–Riemann condition, we obtain the equations

$$(\phi_x, \phi_z, \psi_x, \psi_z) = (x_\phi, z_\phi, x_\psi, z_\psi)/(x_\phi^2 + z_\phi^2). \tag{16}$$

Higher-order derivatives are obtained by a straightforward application of the chain rule. The derivatives $x_\phi, z_\phi, x_{\phi\phi}, z_{\phi\phi}$ are obtained by term-by-term differentiation of (12).

The perturbations are approximated by truncating (5) at M Fourier modes. The unknown coefficients $\{a_n, b_n\}$, $n = -M, \ldots, M$ are chosen to satisfy (4) at $2M+1$ points, spaced in equal arclength increments between adjacent crests of the unperturbed wave. The resulting system of order $4M+2$ is of the form:

$$(\mathbf{A} - \sigma\mathbf{B})\mathbf{u} = 0, \tag{17}$$

where $\mathbf{u} = \{a_{-M} \ldots a_M, b_{-M} \ldots b_M\}$ and the matrices $\mathbf{A}$ and $\mathbf{B}$ are complex functions of p, q and h/λ. A standard eigenvalue solver (based on the QZ algorithm) is used to find the $4M+2$ eigenvalues of the system (17). Attention is focused on those eigenvalues

h/λ	p	q	M	$\mathscr{R}\sigma$	$\mathscr{I}\sigma$
0·064	0·32	0·00	10	−0·146396	0·013273
			20	−0·146396	0·013273
0·111	0·60	0·00	10	−0·213688	0·023644
			20	−0·213876	0·022701
			30	−0·213873	0·022703
0·111	0·50	1·15	10	0·000278	0·042674
			20	0·000003	0·041263
			30	0·000000	0·041268
0·127	0·50	0·79	20	0·000439	0·086359
			30	−0·000009	0·089338
			40	0·000615	0·088408
0·131	0·50	0·65	30	−0·000113	0·111884
			40	0·010084	0·109837
			45	−0·000516	0·108651
0·131	0·50	0·00	30	−0·000399	0·073644
			40	0·015399	0·063804
			45	−0·000386	0·067337

TABLE 1. Examples of the dependence of the eigenvalues on the truncation.

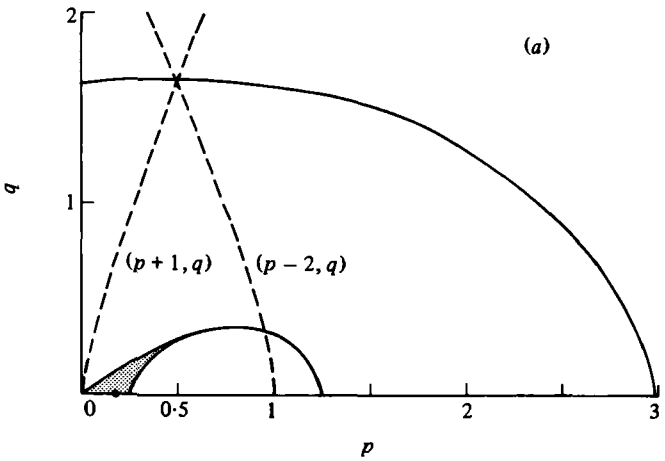

FIGURE 2. Instability regions for $m = 1$. The dot labels the point of maximum instability. The dashed lines are points of neutral stability, labelled by the dominant wavenumber of the eigenfunction. (*a*) $h/\lambda = 0{\cdot}032$, (*b*) $h/\lambda = 0{\cdot}064$, (*c*) $h/\lambda = 0{\cdot}095$, (*d*) $h/\lambda = 0{\cdot}111$, (*e*) $h/\lambda = 0{\cdot}127$, (*f*) $h/\lambda = 0{\cdot}131$.

which have a non-zero imaginary part. The truncation M is increased until the eigenvalues have converged. The accuracy of the eigenvalues can be tested by increasing M, and by checking that the last components of the corresponding eigenvector are sufficiently small. For $h/\lambda \leqslant 0{\cdot}10$, $M = 20$ is sufficient to obtain the relevant eigenvalues to three significant figures. Up to $h/\lambda = 0{\cdot}127$, the eigenvalues can accurately be obtained using $M = 40$. For $h/\lambda = 0{\cdot}1305$, $M = 40$ was used and comparisons were made with $M = 45$. For this wave steepness, the quantitative accuracy is poor, but qualitative features should be adequately obtained. The dependence of the eigenvalue on the truncation is given in table 1.

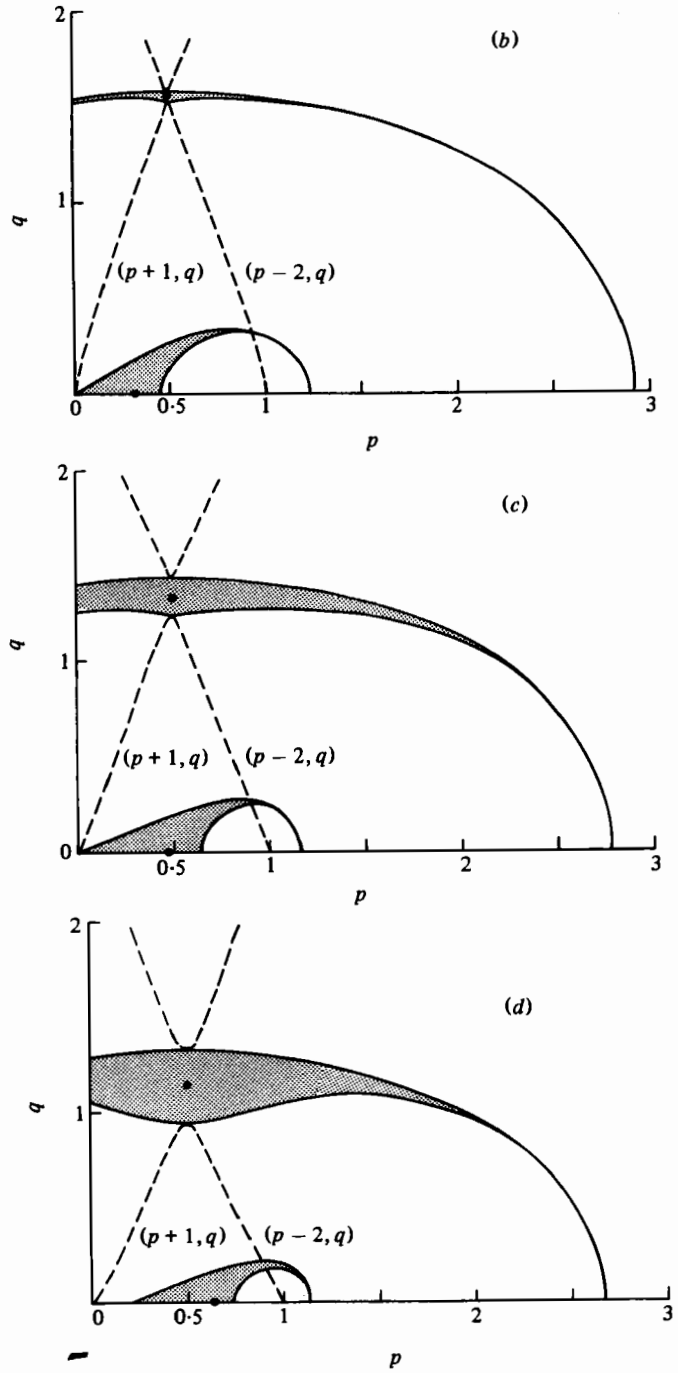

FIGURE 2*b*, *c*, *d*. For legend see p. 320.

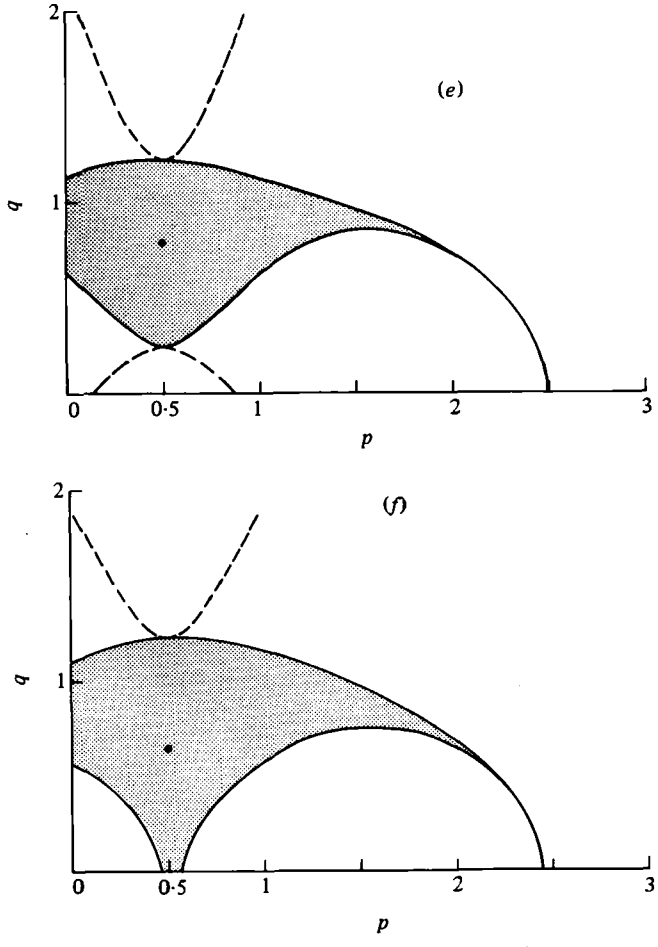

FIGURE 2e,f. For legend see p. 320.

As a check of the eigenvalue solver, a non-singular system can be constructed from the system (17), with the eigenvalue as an unknown, and using a normalization condition as an extra equation. We have the nonlinear system

$$(\mathbf{A} - \sigma \mathbf{B})\,\mathbf{u} = 0, \quad \mathbf{u}^*\mathbf{u} = 1. \tag{18}$$

This system of $4N + 3$ equations can be solved by Newton's method using the solution from the QZ algorithm as an initial guess of the $4N + 3$ unknowns $\{\mathbf{u}, \sigma\}$. In all cases, the Newton method confirmed the accuracy of the eigenvalue solver.

All computations were performed in double precision (14 digits) on a Prime 750 minicomputer. For $M = 20$, the eigenvalues are obtained in about 6 min. For $M = 40$, the eigenvalues of the resulting 162×162 complex matrix are obtained in about 30 min, with a substantial amount of that time required for paging through virtual memory.

	Class I, $m = 1$				Class II, $m = 1$			
h/λ	p	q	$\mathscr{R}\sigma$	$\mathscr{I}\sigma$	p	q	$\mathscr{R}\sigma$	$\mathscr{I}\sigma$
inf	$2ka$	0	$-ka$	$\frac{1}{2}(ka)^2$	0·5	$q_0 - 3{\cdot}2(ka)^2$	0	$0{\cdot}59(ka)^3$
0·032	0·18	0	−0·086	$4{\cdot}09 \times 10^{-3}$	0·5	1·64	0	$6{\cdot}00 \times 10^{-4}$
0·064	0·32	0	−0·146	$1{\cdot}33 \times 10^{-2}$	0·5	1·54	0	$5{\cdot}23 \times 10^{-3}$
0·095	0·47	0	−0·189	$2{\cdot}26 \times 10^{-2}$	0·5	1·33	0	$2{\cdot}15 \times 10^{-2}$
0·111	0·60	0	−0·214	$2{\cdot}27 \times 10^{-2}$	0·5	1·15	0	$4{\cdot}13 \times 10^{-2}$
0·127	—	—	Stable	—	0·5	0·79	0	$8{\cdot}88 \times 10^{-2}$
0·131	—	—	Stable	—	0·5	0·65	0	$1{\cdot}1 \times 10^{-1}$
0·131	—	—	Stable	—	0·5	0·00	0	$6{\cdot}7 \times 10^{-2}$

TABLE 2. The maximum growth rate as a function of wave steepness. $ka = \pi(h/\lambda)$. The first row gives results for $h/\lambda \ll 1$. $q_0 = \frac{3}{4}\sqrt{5}$.

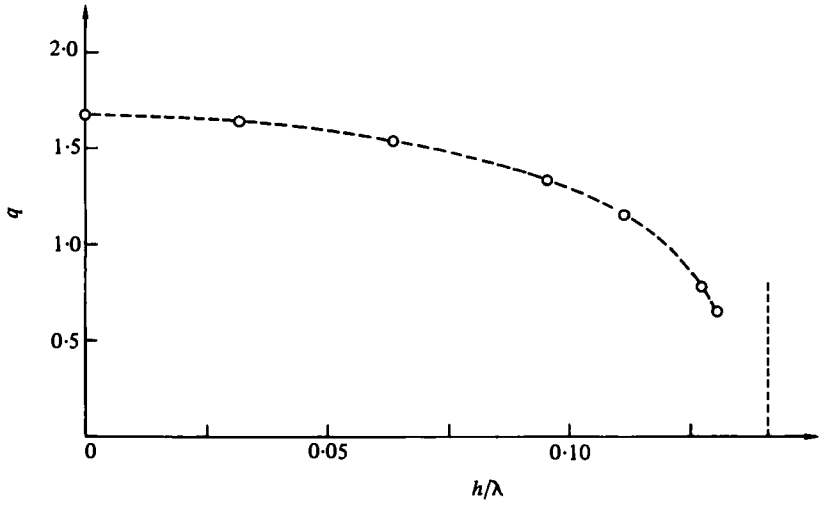

FIGURE 3. The transverse wavenumber of the dominant class II instability as a function of wave steepness. The dashed line on the right represents the highest wave.

4. Results

The instability regions corresponding to the first members of the two classes are plotted in figure 2 for various values of the wave steepness. The corresponding growth rates are given in table 2. For $q = 0$, $p = O(h/\lambda)$, the class I, $m = 1$ instability has a growth rate $\mathscr{I}\sigma = O((h/\lambda)^2)$ for small h/λ, in agreement with the perturbation analysis of Benjamin & Feir. The instability near $p = \frac{5}{4}$ has a growth rate $O((h/\lambda)^4)$. For larger values of h/λ, the unstable region continues to grow until $h/\lambda \simeq 0{\cdot}108$, when the region detaches from the origin. Beyond this, the region shrinks as h/λ increases, finally disappearing for $h/\lambda \simeq 0{\cdot}123$. Throughout this range of wave steepness, the maximum instability is attained for $q = 0$, so this instability is predominantly two-dimensional. Recall that the unstable eigenvector has dominant components at $k_x = p + 1$ and $k_x = p - 1$.

The class II, $m = 1$ instability is new. Near $p = 3, q = 0$, the growth rate is $O((h/\lambda)^5)$,

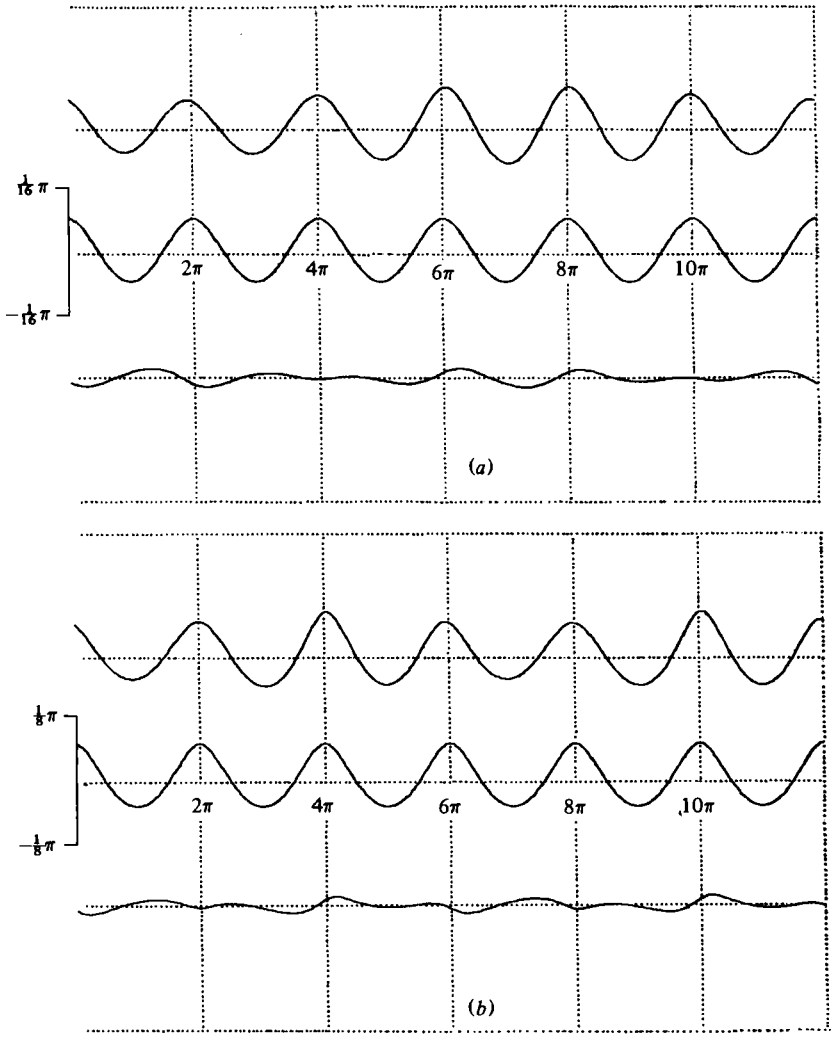

FIGURE 4. The unperturbed wave and the eigenfunction corresponding to the most unstable disturbance of class I. The middle curve is the unperturbed wave, the lower curve is the eigenfunction, and the upper curve is the resulting profile. The eigenfunction has been normalized so that its crest-to-trough height is 0·3 times the crest-to-trough height of the unperturbed wave. Note: the vertical scales have been exaggerated for presentation. (*a*) $h/\lambda = 0{\cdot}032$; (*b*) $h/\lambda = 0{\cdot}064$; (*c*) $h/\lambda = 0{\cdot}095$; (*d*) $h/\lambda = 0{\cdot}111$.

while, near $p = \frac{1}{2}$, $q = \frac{3}{4}\sqrt{5}$, the growth rate is $O((h/\lambda)^3)$. Thus, this instability is initially weaker than the class I resonance. The corresponding eigenvector has dominant components at $k_x = p+1$ and $k_x = p-2$ so, for $p = \frac{1}{2}$, the dominant wavenumber is $\pm\frac{3}{2}$. The maximum growth rate occurs at $p = \frac{1}{2}$, $q \neq 0$, so this instability is strictly three-dimensional. At $h/\lambda \simeq 0{\cdot}10$, the growth rate of this instability becomes larger than the growth rate of the class I instability, and the most unstable disturbance switches from the two-dimensional Benjamin–Feir type to this three-dimensional perturbation. At $h/\lambda \simeq 0{\cdot}129$, the instability region touches the p-axis yielding a two-dimensional unstable disturbance, which was initially identified by Longuet-Higgins

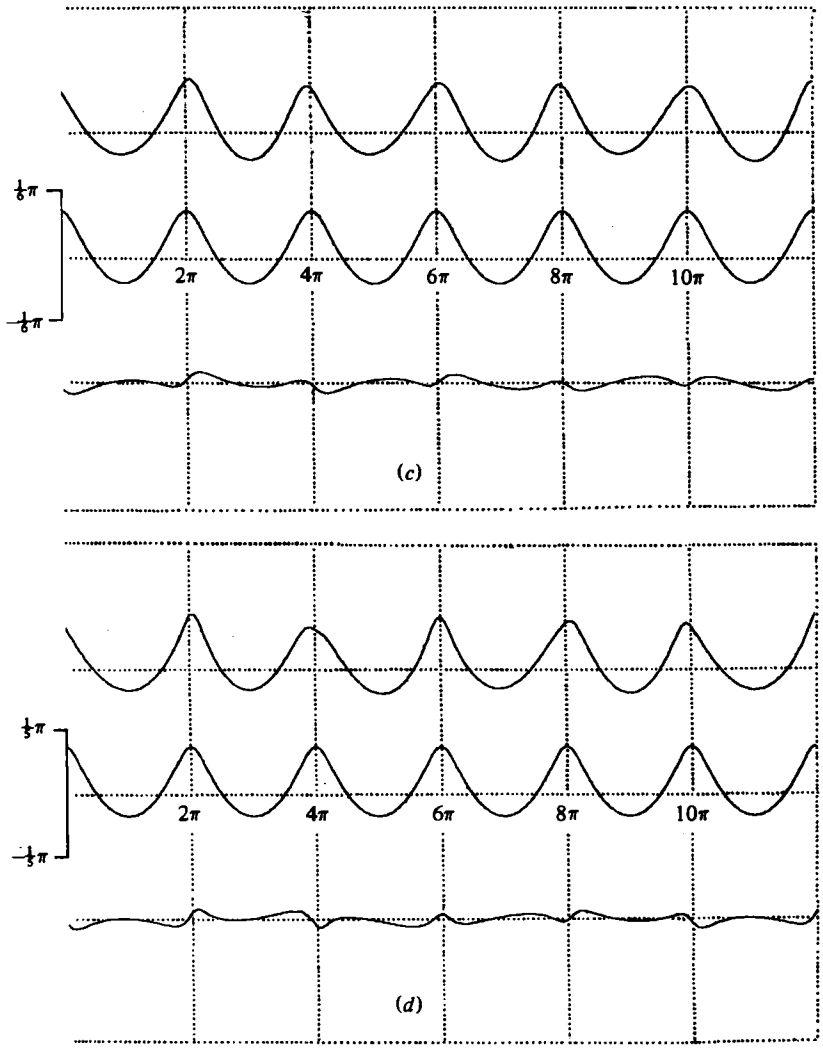

FIGURE 4*c*, *d*. For legend see p. 324.

(1978*a*). It should be noted, however, that the strongest disturbance occurs for $q \neq 0$ and is three-dimensional; see figure 3.

The point of maximum instability for the class II resonance occurs with $\mathscr{R}\sigma = 0$; thus the perturbation remains stationary (but increasing in amplitude) in a frame of reference moving with the unperturbed wave. In fact, $\mathscr{R}\sigma = 0$ along the line $p = \frac{1}{2}$ in the unstable region, so at the stability boundary we have $\sigma = 0$, and the perturbation is a neutral disturbance. This suggests the possibility that the unperturbed wave can bifurcate into a steady three-dimensional wave pattern. Indeed, this neutral stability point touches the p-axis at $h/\lambda = 0{\cdot}129$, in good agreement with the value found by Chen & Saffman (1980) for two-dimensional bifurcation of a Stokes wave train. Values of p and q corresponding to neutral disturbance have been plotted in figure 2.

In figure 4, the unperturbed wave, the eigenfunction corresponding to the most unstable disturbance, and the resultant profile is plotted for class I, $m = 1$. Since in general p is not rational, these perturbations are not strictly periodic. The

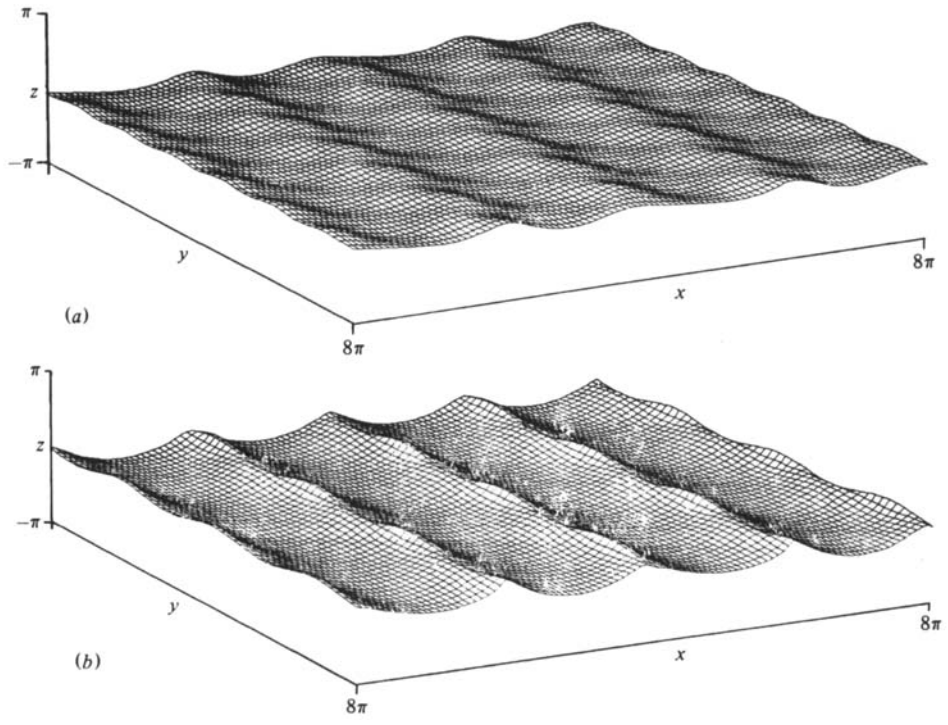

FIGURE 5. The perturbed wave corresponding to the most unstable disturbance of class II. The eigenfunction is normalized as in figure 3. (*a*) $h/\lambda = 0{\cdot}064$, (*b*) $h/\lambda = 0{\cdot}127$.

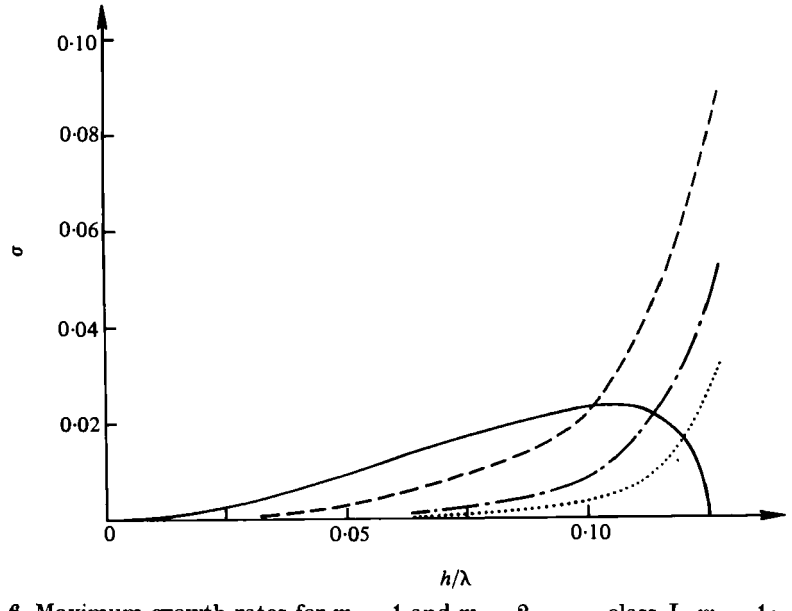

FIGURE 6. Maximum growth rates for $m = 1$ and $m = 2$. ——, class I, $m = 1$; - - -, class II, $m = 1$; — - —, class I, $m = 2$; . . . . ., class II, $m = 2$.

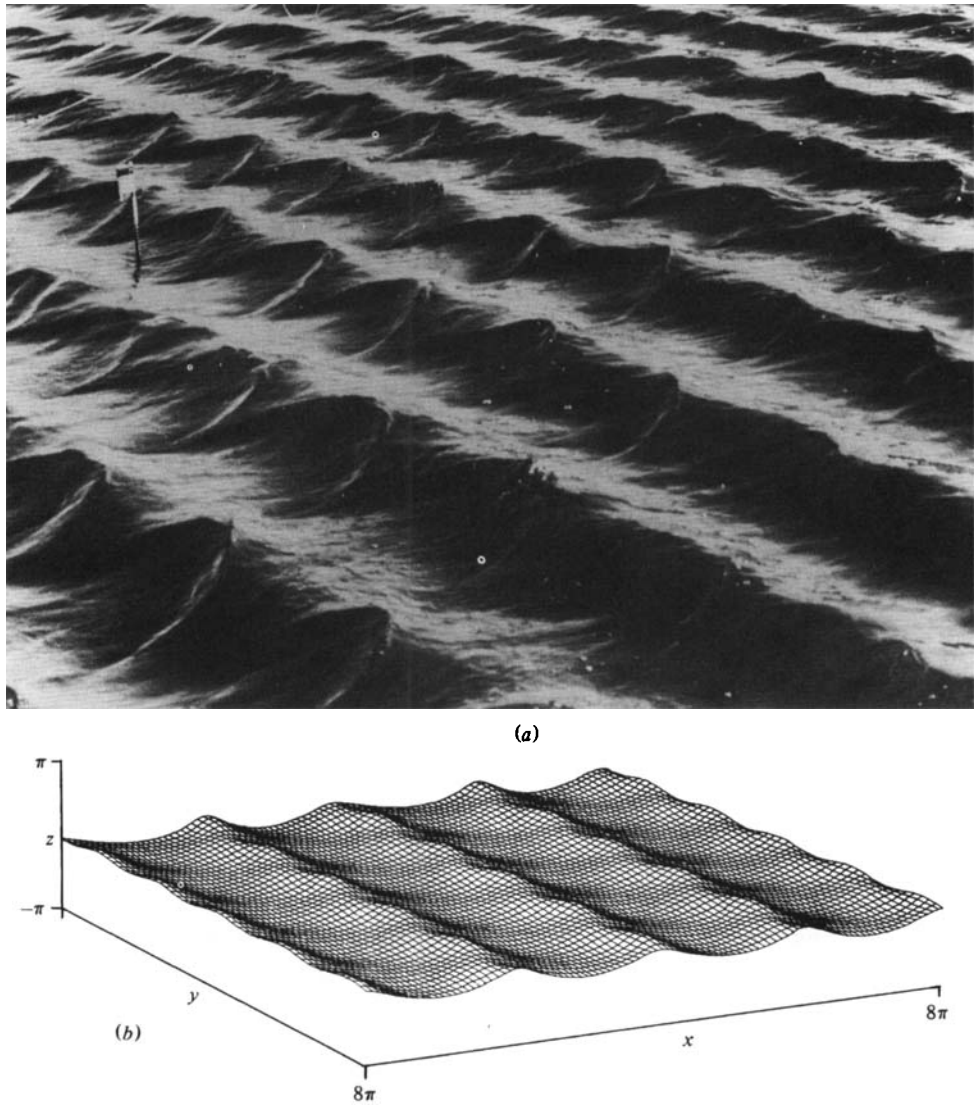

FIGURE 7. Comparison of theory and experiment for $h/\lambda = 0{\cdot}105$. (*a*) Photograph by Su (1981), (*b*) perturbed wave (theory). The eigenfunction is normalized as in figure 3.

eigenfunction is arbitrary up to multiplication by a complex number, thus the phase and crest-to-trough height is undetermined. Since the class I, $m = 1$ eigenvalue has $\mathscr{R}\sigma \neq 0$, the choice of phase corresponds to fixing the origin in time. Figure 4 represents the profile at one instant in time. The profile will distort as time increases. In figure 5, the situation corresponding to class II, $m = 1$, is plotted. Since the maximum disturbance occurs for $p = \frac{1}{2}$ and has $\mathscr{R}\sigma = 0$, the perturbation is periodic and moves with the unperturbed wave. The disturbance is three-dimensional ($q \neq 0$); thus the choice of phase defines the origin of the y-axis.

The trends exhibited by $m = 1$ of classes I and II are reflected in the higher-order interactions. For $m = 2$, class I, the maximum growth rate occurs for $p = 0$, $q \neq 0$, and has a growth rate $\mathscr{I}\sigma = O((h/\lambda)^4)$ for small values of the wave steepness. For $m = 2$,

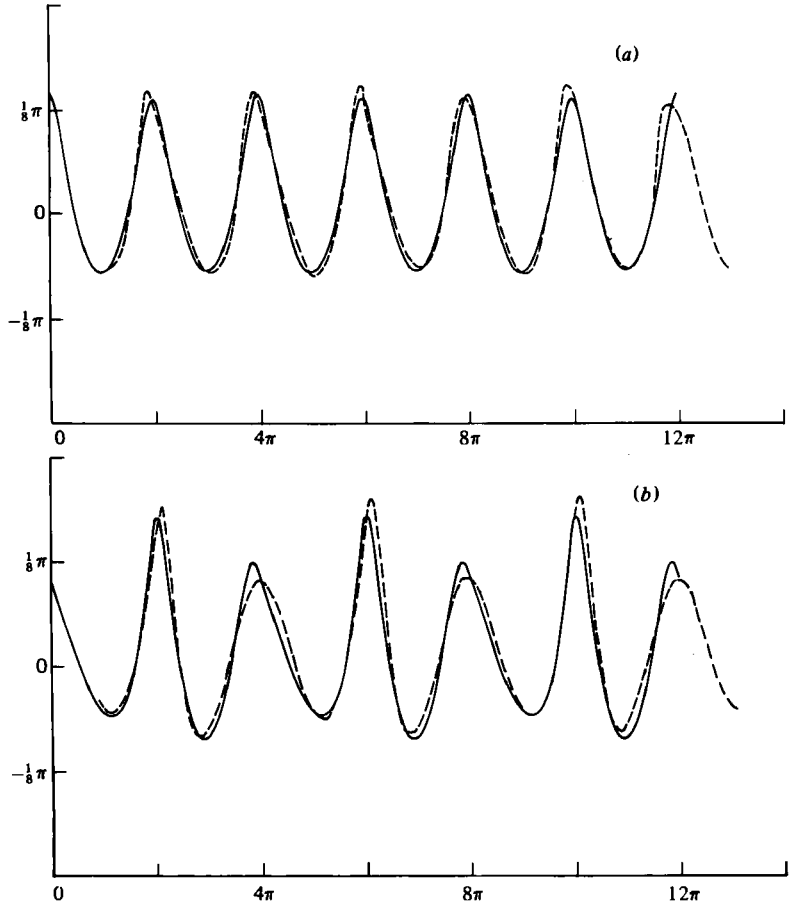

FIGURE 8. Comparison of wave profiles of figure 3. Dashed curve is the experimental measurement (Su 1981); solid curve is the calculated profile. (*a*) $y = 0$, (*b*) $y = \frac{1}{4}\pi$.

class II, the point of maximum instability occurs at $p = \frac{1}{2}$, $q \neq 0$ and has an initial growth rate of $O((h/\lambda)^5)$. The maximum instability in these cases occurs with $\mathscr{R}\sigma = 0$. For the range of wave heights considered here, $0 < h/\lambda < 0{\cdot}1305$, the $m = 1$ interactions produce the dominant instabilities. Comparison of the growth rates for the various instabilities is given in figure 6.

Based on the results of $m = 1$ and $m = 2$, we draw the following conclusions:

(i) For $m = 1$ (class I), the strongest instability occurs at $p \neq 0$, $q = 0$. For class I, $m > 1$, the most unstable disturbance occurs at $p = 0, q \neq 0$. For class II, the maximum instability occurs at $p = 0{\cdot}5$, $q \neq 0$.

(ii) Except for class I, $m = 1$, the most unstable disturbance occurs with $\mathscr{R}\sigma = 0$; thus the phase is stationary in a frame of reference moving with the unperturbed wave. The stability boundary at $p = 0$ (class I) or $p = 0{\cdot}5$ (class II) is a point of neutral stability $\sigma = 0$, and may represent a bifurcation into a steady three-dimensional wave pattern.

(iii) In terms of the N-fold resonance interpretation, $\omega_1 = -\omega_2 + N\omega_0$, the instability has a maximum growth rate $\mathscr{I}\sigma = O((h/\lambda)^N)$ for small h/λ.

5. Comparison with observation

The perturbation analysis of Benjamin & Feir (1967) afforded an explanation of the observation that a gravity wave is unstable to two-dimensional perturbations. Improvements of the theory based on the nonlinear equations led to good agreement with experiment (Longuet-Higgins 1978*a*). It is significant to note that the original experiments were for values of the wave steepness $h/\lambda < 0{\cdot}054$, a range in which the three-dimensional instabilities are quite weak.

Recent experiments on steep waves have noted the tendency for the wave train to disintegrate as a result of three-dimensional perturbations for $h/\lambda > 0{\cdot}08$ (Su 1981). For the experimental value $h/\lambda = 0{\cdot}105$, Su measured the wavelength of the perturbation to be $\lambda_x = 2{\cdot}1\,\mathrm{m}$, $\lambda_y = 0{\cdot}915\,\mathrm{m}$, yielding $k_y/k_x = 2{\cdot}36$. At this steepness, the present calculation predicts that the most unstable disturbance will occur for $p = \frac{1}{2}$, $q = 1{\cdot}23$, yielding $k_y/k_x = 2{\cdot}46$, in good agreement with the experimental value. The wave profiles are compared in figure 7 and 8, where the amplitude of the eigenfunction (which is undetermined by the linearized equations) has been chosen for the best agreement with the experimental profile. The numerical calculations yield $\mathscr{I}\sigma = 0{\cdot}0316$, but experimental data on the growth rate is presently not available for comparison.

6. Conclusions

It has been shown that the coincidence of eigenvalues given by the linear dispersion relation leads to instability for finite amplitude. For small wave steepness, the most unstable disturbance is two-dimensional while, for steeper waves, the instability is predominantly three-dimensional. This result has been used to explain the observation that steep waves collapse as a result of three-dimensional perturbations.

The resonance curves also suggest the existence of a family of two-dimensional instabilities for $p = m^2 + \frac{1}{4}$ (class I) and $p = m^2 + m + 1$ (class II). Although these instabilities are weak, it is significant that these superharmonic instabilities are missed by conventional WKB analysis (Dagan 1975; Phillips 1981), but are suggested by analogy with instabilities of Hill's equation (Hasselmann 1979). This instability is not in conflict with the conclusion of Longuet-Higgins that there are no unstable superharmonic disturbances, since these perturbations are not strictly periodic, and are thus not allowed by his analysis.

The possibility of further instability regions which do not exist for small h/λ cannot be excluded, but we have found no evidence of additional instabilities.

We have also identified some neutral disturbances ($\sigma = 0$), which are possible bifurcations of the two-dimensional wave train. Recent investigations have obtained two-dimensional bifurcations of the Stokes wave (Chen & Saffman 1979), and three-dimensional bifurcations in the Zakharov equation (Saffman & Yuen 1980). A study is presently under way on three-dimensional bifurcations based on the full nonlinear equations.

The author wishes to thank Dr M. Y. Su for permission to use his photograph, and Professor P. G. Saffman and Dr H. C. Yuen for many valuable comments and suggestions during the course of the research and preparation of the manuscript.

REFERENCES

BENJAMIN, T. B. & FEIR, J. E. 1967 The disintegration of wavetrains on deep water. *J. Fluid Mech.* **27**, 417–430.

CHEN, B. & SAFFMAN, P. G. 1980 Numerical evidence for the existence of new types of gravity waves of permanent form on deep water. *Stud. Appl. Math.* **62**, 1–21.

COKELET, E. D. 1977 Steep gravity waves in water of uniform arbitrary depth. *Phil. Trans. R. Soc. Lond.* A **286**, 184–230.

CRAWFORD, D. R., LAKE, B. M., SAFFMANN, P. G. & YUEN, H. C. 1981 Stability of weakly nonlinear deep-water waves in two and three dimensions. *J. Fluid Mech.* **105**, 177–192.

DAGAN, G. 1975 Taylor instability of a non-uniform free-surface flow. *J. Fluid Mech.* **67**, 113–123.

HASSELMANN, D. E. 1979 The high wavenumber instabilities of a Stokes wave. *J. Fluid Mech.* **93**, 491–500.

LIGHTHILL, M. J. 1965 Contributions to the theory of waves in nonlinear dispersive systems. *J. Inst. Math. Appl.* **1**, 269–306.

LONGUET-HIGGINS, M. S. 1978*a* The instabilities of gravity waves of finite amplitude in deep water. II. Subharmonics. *Proc. R. Soc. Lond.* A **360**, 489–505.

LONGUET-HIGGINS, M. S. 1978*b* Some new relations between Stokes coefficients in the theory of gravity waves. *J. Inst. Math. Applic.* **22**, 261–273.

MCLEAN, J. W., MA, Y. C., MARTIN, D. U., SAFFMAN, P. G. & YUEN, H. C. 1981 Three-dimensional instability of finite amplitude water waves. *Phys. Rev. Lett.* **46**, 817–820.

PHILLIPS, O. M. 1960 On the dynamics of unsteady gravity waves of finite amplitude. *J. Fluid Mech.* **9**, 193–217.

PHILLIPS, O. M. 1981 The dispersion of short wavelets in the presence of a dominant long wave. Unpublished manuscript.

SAFFMAN, P. G. 1980 Long wavelength bifurcation of gravity waves on deep water. *J. Fluid Mech.* **101**, 567–581.

SAFFMAN, P. G. & YUEN, H. C. 1980 A new type of three-dimensional deep-water wave of permanent form. *J. Fluid Mech.* **101**, 797–808.

SCHWARTZ, L. W. 1974 Computer extension and an analytic continuation of Stokes expansion for gravity waves. *J. Fluid Mech.* **62**, 553–578.

SU, M. Y. 1981 Three-dimensional deep-water waves. Part I. Laboratory experiments on spilling breakers. Unpublished manuscript.

ZAKHAROV, Y. E. 1968 Stability of periodic waves of finite amplitude on the surface of a deep fluid. *J. Appl. Mech. Tech. Phys.* **2**, 190–194.